



Synthesis, spectroscopy, electrochemistry and thermal study of vanadyl unsymmetrical Schiff base complexes

Ali Hossein Kianfar^{a,*}, Vida Sobhani^a, Morteza Dostani^a, Mojtaba Shamsipur^b, Mahmoud Roushani^b

^a Department of Chemistry, Yasouj University, Daneshjoo Street, 75914-353 Yasouj, Iran

^b Department of Chemistry, Razi University, Kermanshah, Iran

ARTICLE INFO

Article history:

Received 16 June 2010

Received in revised form 13 August 2010

Accepted 21 August 2010

Keywords:

Vanadyl complexes
Schiff base complexes
Thermogravimetry
Electrochemistry

ABSTRACT

The new tetradentate unsymmetrical N_2O_2 Schiff base ligands and VO(IV) complexes were synthesised and characterized by using IR, UV–Vis and elemental analysis. The electrochemical properties of the vanadyl complexes were investigated by means of cyclic voltammetry. The oxidation potentials are increased by increasing the electron-withdrawing properties of functional groups of the Schiff base ligands according to the trend of $MeO < H < Br < NO_2$. The thermogravimetry (TG) and differential thermoanalysis (DTA) of the VO(IV) complexes were carried out in the range of 20–700 °C. The complexes were decomposed in two stages. Also decomposition of synthesised complexes is related to the Schiff base characteristics. The thermal decomposition of the studied reactions was first order.

© 2010 Elsevier B.V. All rights reserved.

1. Introduction

The high stability potential of Schiff base complexes with different oxidation states extended the application of these compounds in a wide range. The complexes studied were known as catalysts in organic redox and electrochemical reduction reactions [1–4]. Knowledge of electronic and steric effects to control the redox chemistry of these compounds may prove to be critical in designing new catalysts. The vanadyl Schiff base complexes play an important role in this area [5]. Vanadium complexes are very interesting model compounds to clarify several biochemical processes [6,7].

Thermogravimetry (TG) and differential thermoanalysis (DTA) are valuable technics for studying the thermal behaviour of chemical compounds [8–12]. Also the electrochemical methods can be envisioned to provide valuable information on the catalytic processes since catalytic conversions are frequently accompanied with the changes in the structure of complexes and metal oxidation states. The present study describes the electronic influence of salophen derivatives on thermal and electrochemical properties of vanadyl(IV) Schiff base complexes (Fig. 1). The electrochemical properties of the vanadyl complexes were studied by cyclic voltammetry in DMF solvent. Kinetics and thermodynamic

parameters were calculated using Coats and Redfern [13] method.

2. Experimental

2.1. Chemicals and apparatus

All of the chemicals and solvents used for synthesis and electrochemistry were of commercially available reagent grade and used without purification. The elemental analyses were determined by CHN–O–Heraeus elemental analyzer. Infrared spectra were recorded by FT-IR JASCO-680 spectrophotometer in the 4000–400 cm^{-1} . UV–Vis spectra were recorded by means of JASCO V-570 spectrophotometer in the range of 190–900 nm. The 1H NMR spectra were recorded in $DMSO-d_6$ solvent by DPX-400 MHz FT-NMR. Thermogravimetry (TG) and differential thermoanalysis (DTA) were carried out by using a PL-1500. The measurements were performed in air atmosphere. The heating rate was held at 10 °C min^{-1} .

Cyclic voltammograms were performed by using an autolab modelar electrochemical system (ECO Chemie, Utrecht, The Netherlands) equipped with a PSTA 20 module and driven by GPES (ECO Chemie) in conjunction with a three-electrode system and a PC for data processing. An Ag/AgCl (saturated KCl)/3 M KCl reference electrode, a Pt wire as counter electrode and a glassy carbon electrode as working electrode (metrom glassy carbon, 0.0314 cm^2) were used for the electrochemical studies. Voltammetric measurements were performed at room temperature in DMF solution with

* Corresponding author. Tel./fax: +98 741 2223048.

E-mail addresses: akianfar@mail.yu.ac.ir, asarvestani@yahoo.com (A.H. Kianfar).

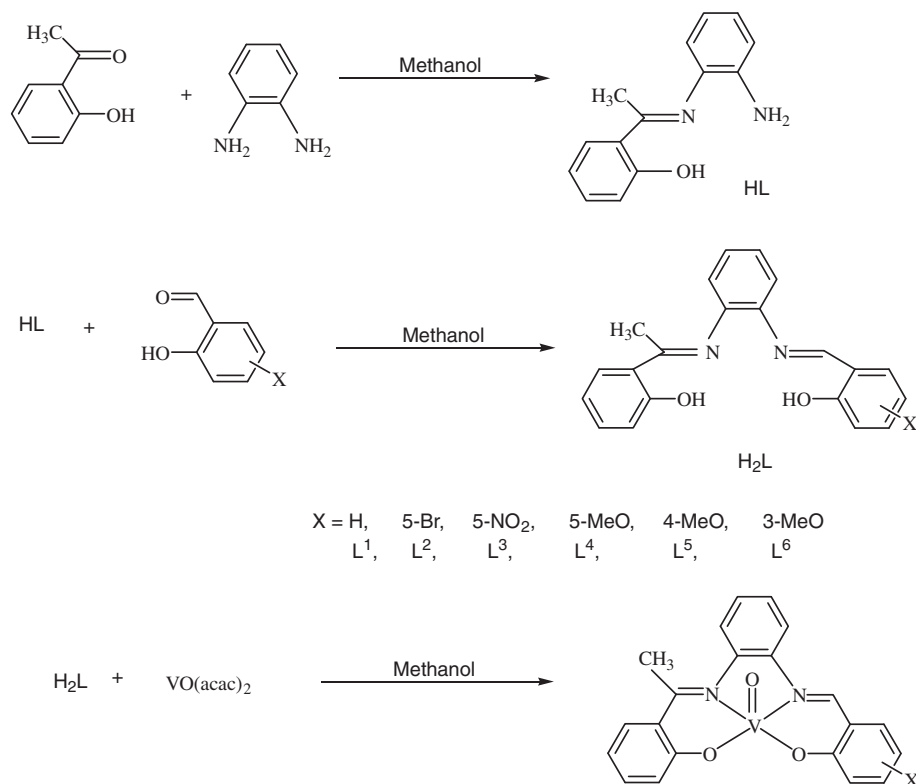


Fig. 1. The structure of Schiff bases and their complexes.

0.1 M tetrabutylammonium perchlorate as the supporting electrolyte.

2.2. Synthesis

The tetradentate Schiff base ligands, L^1 – L^4 , the new L^5 and L^6 were prepared according to the literature [14]. The vanadyl complexes were synthesised by refluxing a methanolic solution of the tetradentate Schiff base ligands and vanadylacetylacetonate. The reaction was continued for 2 h until a green precipitate was obtained. It was filtered, washed with methanol and dried in vacuum.

H_2L^5 yield (80%): ($C_{21}H_{18}N_2O_2$), FT-IR (KBr cm^{-1}) ν_{max} 1635 (C=N), 1504 (C=C), 1222 (C–O). UV-Vis, λ_{max} (nm) (ϵ , $L mol^{-1} cm^{-1}$) ($CHCl_3$): 313 (3400), 278 (7400). 1H NMR (DMSO- d_6 , 400 MHz) $\delta = 2.50$ (s, 3H, CH_3), $\delta = 3.80$ (s, 3H, O- CH_3), $\delta = 6.20$ – 7.80 (m, 11H), $\delta = 9.00$ (s, 1H, HC=N), $\delta = 12.90$ (s, 1H, OH), $\delta = 14.30$ (s, 1H, OH).

H_2L^6 yield (85%): ($C_{21}H_{18}N_2O_2$), FT-IR (KBr cm^{-1}) ν_{max} 1643 (C=N), 1461 (C=C), 1257 (C–O). UV-Vis, λ_{max} (nm) (ϵ , $L mol^{-1} cm^{-1}$) ($CHCl_3$): 343 (14 000), 265 (42 000). 1H NMR (DMSO- d_6 , 400 MHz) $\delta = 2.50$ (s, 3H, CH_3), $\delta = 3.60$ (s, 3H, O- CH_3), $\delta = 6.10$ – 7.50 (m, 11H), $\delta = 9.80$ (s, 1H, HC=N), $\delta = 15.40$ (s, 2H, OH).

VOL^1 yield (80%): Anal. Calc. for $C_{21}H_{16}N_2O_3V$: C, 63.79; H, 4.05; N, 7.08. Found: C, 63.95; H, 4.09; N, 7.12%. FT-IR (KBr cm^{-1}) ν_{max} 1610 (C=N), 976 (V=O). UV-Vis, λ_{max} (nm) (ϵ , $L mol^{-1} cm^{-1}$) (ethanol): 393 (24 500), 320 (27 000), 244 (58 000).

VOL^2 yield (80%): Anal. Calc. for $C_{21}H_{15}BrN_2O_3V$: C, 52.95; H, 3.16; N, 5.90. Found: C, 53.57; H, 3.21; N, 5.98%. FT-IR (KBr cm^{-1}) ν_{max} 1600 (C=N), 981 (V=O). UV-Vis, λ_{max} (nm) (ϵ , $L mol^{-1} cm^{-1}$) (ethanol): 389 (11 500), 320 (13 000), 277 (19 000), 249 (32 000).

VOL^3 yield (85%): Anal. Calc. for $C_{21}H_{15}N_3O_3V$: C, 57.27; H, 3.40; N, 9.54. Found: C, 57.89; H, 3.47; N, 9.83%. FT-IR (KBr cm^{-1}) ν_{max}

1609 (C=N), 1324 (NO_2), 991 (V=O). UV-Vis, λ_{max} (nm) (ϵ , $L mol^{-1} cm^{-1}$) (ethanol): 372 (40 000), 311 (48 000).

VOL^4 yield (85%): Anal. Calc. for $C_{22}H_{18}N_2O_4V$: C, 62.11; H, 4.23; N, 6.58. Found: C, 62.68; H, 4.32; N, 6.87%. FT-IR (KBr cm^{-1}) ν_{max} 1614 (C=N), 1273 (C–O), 980 (V=O). UV-Vis, λ_{max} (nm) (ϵ , $L mol^{-1} cm^{-1}$) (ethanol): 469(sh) (19 000), 397 (29 000), 322 (45 000), 247 (84 000).

VOL^5 yield (80%): Anal. Calc. for $C_{22}H_{18}N_2O_4V$: C, 62.11; H, 4.23; N, 6.58. Found: C, 62.46; H, 3.25; N, 6.65%. FT-IR (KBr cm^{-1}) ν_{max} 1614 (C=N), 1242 (C–O), 978 (V=O). UV-Vis, λ_{max} (nm) (ϵ , $L mol^{-1} cm^{-1}$) (ethanol): 387 (26 000), 325 (21 000), 243 (37 000).

VOL^6 yield (75%): Anal. Calc. for $C_{22}H_{18}N_2O_4V$: C, 62.11; H, 4.23; N, 6.58. Found: C, 62.93; H, 4.28; N, 6.77%. FT-IR (KBr cm^{-1}) ν_{max} 1605 (C=N), 1249 (C–O), 986 (V=O). UV-Vis, λ_{max} (nm) (ϵ , $L mol^{-1} cm^{-1}$) (ethanol): 401 (4200), 342 (65 000), 310 (56 000), 241 (93 000).

3. Results and discussion

3.1. IR characteristics

The IR spectra of the free Schiff base ligands and the complexes show several bands in the 400–4000 cm^{-1} region. The OH stretching frequency of the ligands is observed in the region of 2500–3100 cm^{-1} due to the internal hydrogen bonding vibration (O–H \cdots N). This band disappeared in the spectra of the complexes [11,12,15].

The free ligands have a characteristic C=N bond in 1611–1643 cm^{-1} region. For the Schiff base complexes C=N was observed in 1600–1614 cm^{-1} . The C=N stretching band of the schiff base complexes is generally shifted to a lower frequency, indicating a decrease in the C=N bond order due to the coordinate bond

formation between the metal and the imine nitrogen lone pair [11,12].

The band which appeared at 976–991 cm^{-1} is assigned to $\nu(\text{V}=\text{O})$. This band is observed as a new peak for the complexes and is not observed in the spectrum of free ligands [16,17].

3.2. Electronic spectra

In solution, the electronic spectra of the Schiff base ligands consist of a relatively intense band in the 250–350 nm region, involving $\pi \rightarrow \pi^*$ transition [14]. The vanadyl complexes show an intense CT transition in 380–401 nm regions. Also the $d-d$ transition in this type of complexes appears in the range of 550–900 nm. However, this band does not appear due to the low intensity of the $d-d$ transitions and low solubility of the studied complexes in the above range [18].

3.3. The electrochemical study of vanadyl complexes

The cyclic voltammetry of VOL complexes were carried out in DMF solution at room temperature. A typical cyclic voltammogram of VOL¹ complex in the potential range from 0.0 to 1.0 V (versus Ag/AgCl) is shown in Fig. 2b. An oxidation peak is observed at about Ca. 0.657 V. VOL¹ is oxidized to $[\text{VOL}^1(\text{solvent})]^+$ in a fully reversible one electron step [19]. The electron is removed from the nonbonding orbitals and the V(V) complex is formed. Upon reversal of the scan direction, the V(V) complex is reduced to V(IV) at lower potentials. Multiple scans which resulted in nearly superposable cyclic voltammograms show that the five coordinate geometry is stable in both oxidation states, at least on the cyclic voltammetry time scale. These results revealed that the redox process of all studied vanadyl Schiff base complexes are the one – electron transfer reactions. The oxidation potentials for the different complexes are shown in Table 1. The formal potentials ($E_{1/2}$ (IV/V)) of the V(IV/V) redox couple were calculated as the average of the cathodic (E_{pc}) and anodic (E_{pa}) potentials peak of this process.

To study the effect of functional groups of the Schiff base ligands on the oxidation potentials of [VOL], a series of the vanadyl Schiff base complexes were studied by the cyclic voltammetry method. The results show that the anodic peak potential (E_{pa}) varies as can be expected from the electronic effects of the substituents at positions five. Thus, E_{pa} becomes more positive according to the sequence $\text{MeO} < \text{H} < \text{Br} < \text{NO}_2$. Similar results have been reported for analogous vanadyl(IV), copper(II), nickel(II) and cobalt(III) systems, and have been interpreted assuming that the strong electron-withdrawing effects stabilize the lower oxidation

Table 1

Redox potential data of vanadyl complexes in DMF solution.

Compounds	E_{pa} (V → IV)	E_{pc} (IV → V)	$E_{1/2}$ (IV ↔ V)
VOL ¹	0.657	0.405	0.531
VOL ²	0.684	0.495	0.589
VOL ³	0.774	0.603	0.688
VOL ⁴	0.612	0.396	0.504
VOL ⁵	0.693	0.450	0.571
VOL ⁶	0.666	0.414	0.540

state while the electro-donating groups have a reverse effect [19–23]. Hammett type relationship has been found between the E_{pa} values and the appropriate para-substituent parameters [24], which reflect the variation of the electrode potential as a function of the electron-withdrawing ability of the substituent at positions five (Fig. 3).

To investigate the effect of functional group on different positions, the electrochemical property of complexes with 5-MeO, 3-MeO and 4-MeO functional groups were studied (Fig. 4). The anodic peak potentials increased in the trend of 5-MeO < 3-MeO < 4-MeO. The substituted functional groups of 5-MeO and 3-MeO are electron donors, while the meta-substituted group (4-MeO) is as an electron acceptor by induction effect. Also the methoxy group on the ortho situation has shown a steric hinderance.

3.4. Thermal analysis

The thermal decomposition of the studied complexes presented pathways which depend on the nature of the ligands. These pathways are observed in the TG/DTA curves (Fig. 5). All TG and DTA figures of the other compounds have the same trend. The absence of weight loss up to 80 °C indicates that the crystalline solids have no water molecule. Also, in the studied complexes, the TG showed no weight loss up to 150 °C indicating the absence of water molecule coordinated to complexes [11,12]. All the complexes were decomposed in two steps (Figs. 5 and 6). The temperature range and the percent of loss weight calculated and found for two steps are presented in Table 2. For all the complexes, the first step occurs between 280 and 370 °C. The second step of the thermal decomposition which results in the formation of the V₂O₅ occurs in the range 370–450 °C [8].

3.5. Kinetics aspects

All the well-defined stages were selected to study the decomposition kinetics of the complexes. The kinetics parameters (the acti-

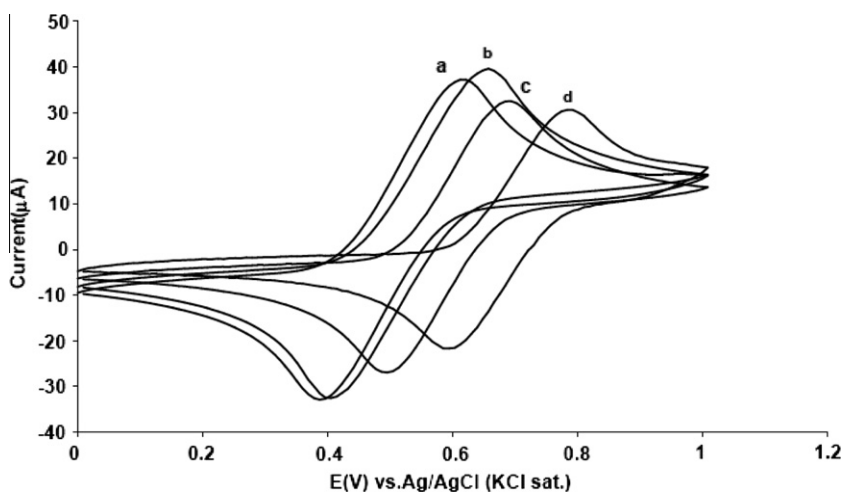


Fig. 2. Cyclic voltammograms of VOL, in DMF at room temperature. Scan rate: 100 mV/s. a = L⁴, b = L¹, c = L², d = L³.

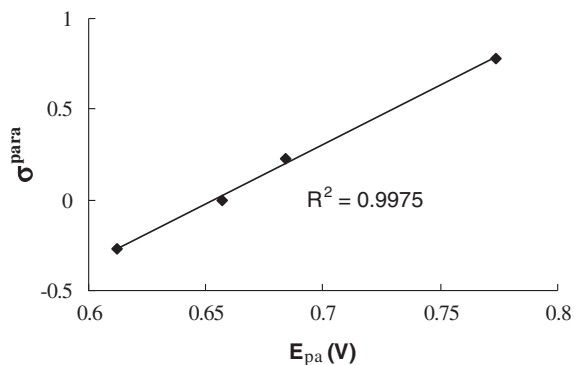


Fig. 3. Correlation between the E_{pa} values for Schiff bases (L^1 – L^4) and the respective σ_{pa} substituent.

vation energy E_a and the pre-exponential factor A) were calculated using the Coats–Redfern equation [13]

$$\log \left[\frac{g(\alpha)}{T^2} \right] = \log \frac{AR}{\phi E} \left[1 - \frac{2RT}{E_a} \right] - \frac{E_a}{2.303RT} \quad (1)$$

where $g(\alpha) = [(W_f)/(W_f - W)]$, W_f is the mass loss upon the completion of the reaction, W is the mass loss up to temperature T , R is the gas constant, E_a is the activation energy and ϕ is heating rate. In the present case, a plot of left hand-side (L.H.S) of this equation versus $1/T$ gives straight line (Fig. 7) whose slope and intercept are used to calculate the kinetics parameters by the least square method. The goodness of fit was checked by calculating the correlation coefficient. The other systems and their steps show the same trend.

The entropy of activation S^\ddagger was calculated using the equation

$$A = \frac{kT_s}{h} e^{\frac{S^\ddagger}{R}} \quad (2)$$

where k , h and T_s are the Boltzmann's constant, the Planck's constant and the peak temperature, respectively. The enthalpy and free energy of activation were calculated using equations

$$E_a = H^\ddagger + RT, \quad (3)$$

$$G^\ddagger = H^\ddagger - TS^\ddagger \quad (4)$$

The various kinetics parameters calculated are given in Table 2. The activation energy (E_a) in the different stages is in the range of 119–376 kJ mol⁻¹. The respective values of the pre-exponential factor

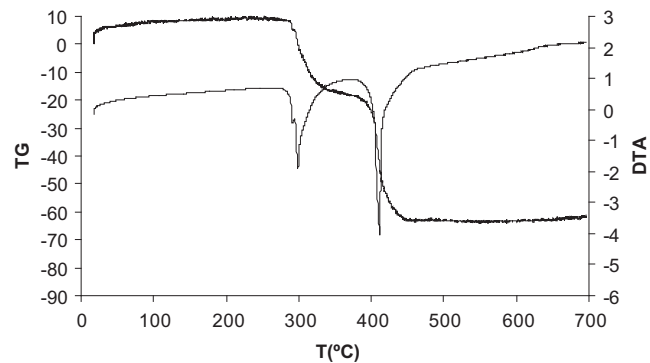


Fig. 5. The TG and DTA of VOL^6 complex.

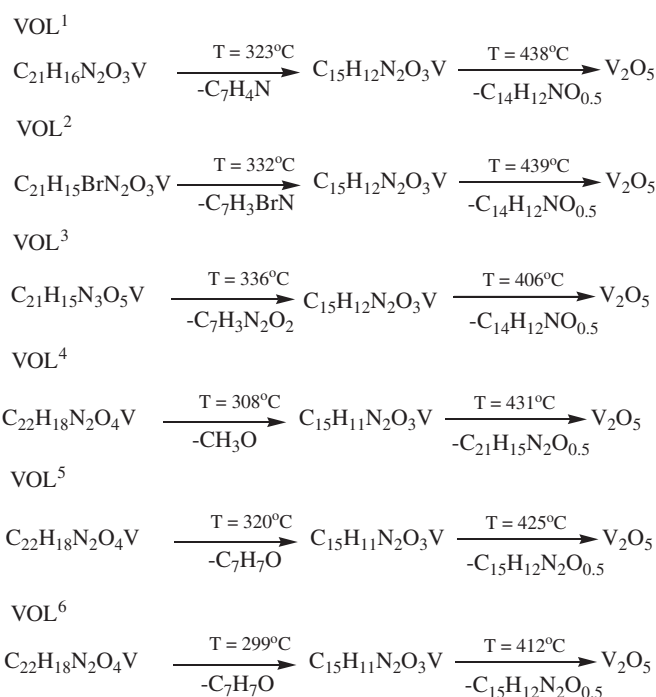


Fig. 6. The TG decomposition pathway the vanadyl Schiff base complexes.

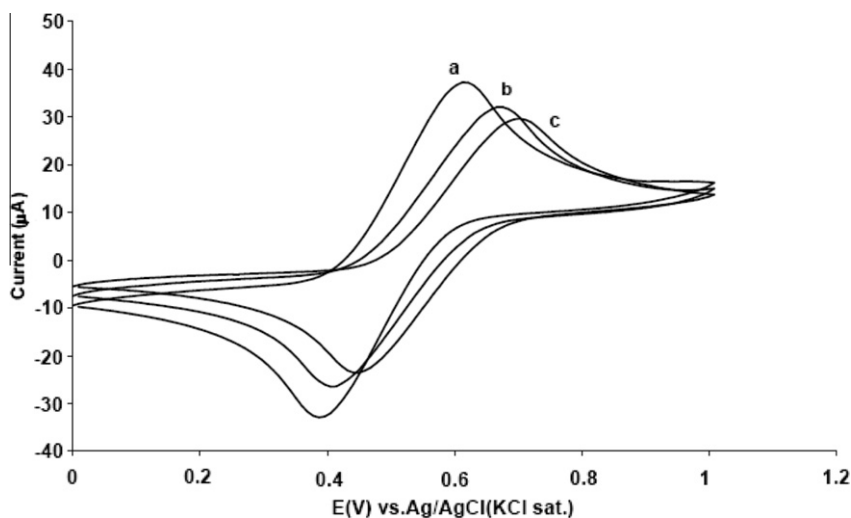


Fig. 4. Cyclic voltammograms of VOL, in DMF at room temperature. Scan rate: 100 mV/s. a = L^4 , b = L^5 , c = L^5 .

Table 2
Thermal and kinetics parameters for vanadyl complexes.

Compounds	ΔT (°C) ^a	Percent (%) ^b	E_a (kJ/mol)	A (s ⁻¹)	S^\ddagger (kJ mol ⁻¹ K ⁻¹)	H^\ddagger (kJ/mol)	G^\ddagger (kJ/mol)
VOL ¹	300–360	26(25)	253.58	4.47×10^{19}	127	249.99	178.81
	380–450	51(51)	213.41	$2.32 \cdot 10^{15}$	41	207.11	176.19
VOL ²	290–370	38(40)	292.54	3.44×10^{22}	108	287.95	188.09
	385–430	42(45)	119.57	3.03×10^{08}	-90	113.27	182.57
VOL ³	300–365	33(32)	282.80	1.01×10^{22}	171	278.21	184.21
	375–455	45(45)	151.50	4.80×10^{10}	-48	145.20	181.74
VOL ⁴	280–350	7.5(9)	231.24	164×10^{18}	98	226.15	172.24
	370–430	68(65)	259.15	8.14×10^{18}	10	252.84	170.09
VOL ⁵	280–360	25(27)	244.56	1.83×10^{19}	119	239.97	173.92
	380–430	53(55)	185.12	3.49×10^{13}	6	178.82	174.52
VOL ⁶	280–355	25(26)	376.26	2.67×10^{31}	352	371.67	178.42
	370–450	53(47)	264.91	5.17×10^{19}	125	258.61	163.85

^a The temperature range of decomposition pathways.

^b Present of weight lose calculated (found).

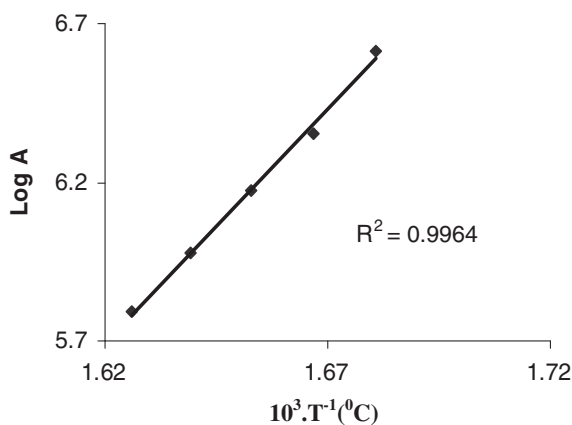


Fig. 7. Coats-Redfern plots of VOL² complex, step 2, $A = \frac{\log \frac{w_f}{w-w_f}}{T^2}$.

(A) vary from 3.03×10^8 to 2.67×10^{31} s⁻¹. The corresponding values of the entropy of activation (S^\ddagger) were in the range of -90 to +352 J mol⁻¹. The enthalpy of activation (H^\ddagger) values were in the range of 113–371 kJ mol⁻¹. The corresponding values of the free energy of activation (G^\ddagger) were in the range of 163–188 kJ mol⁻¹. There was no definite trend in the values of activation parameters among the different stages in the present series. However, due to the unstable intermediate the activation energy of the second stage

was smaller than that of the first one, and occurred at the later stages.

References

- [1] L. Canali, D.C. Sherrington, *Chem. Soc. Rev.* 28 (1998) 85.
- [2] A.A. Isse, A. Gennaro, E. Vianello, *J. Electroanal. Chem.* 444 (1998) 241.
- [3] D. Pletcher, H. Thompson, *J. Electroanal. Chem.* 464 (1999) 168.
- [4] T. Okada, K. Katou, T. Hirose, M. Yuasa, I. Sekine, *J. Electrochem. Soc.* 146 (1999) 2562.
- [5] V. Conte, B. Floris, *Inorg. Chem. Acta* 363 (2010) 1935.
- [6] D. Rehder, *Angew. Chem., Int. Ed.* 30 (1991) 148.
- [7] A. Butler, C.J. Carrano, *Coord. Chem. Rev.* 109 (1991) 152.
- [8] E.A. Pedro, M.S. João, R. Sandra, A.R. Luiz, P.S. Mirian, R.D. Edward, T.G.C. Eder, *Thermochim. Acta* 453 (2007) 9.
- [9] A.A. Soliman, W. Linert, *Thermochim. Acta* 338 (1999) 67.
- [10] A.A. Soliman, *J. Therm. Anal. Calorim.* 63 (2001) 221.
- [11] B.S. Garg, D.N. Kumar, *Spectrochim. Acta, Part A* 59 (2003) 229.
- [12] A. Anthonysamy, S. Balasubramanian, *Inorg. Chem. Commun.* 8 (2005) 908.
- [13] A.W. Coats, J.P. Redfern, *Nature* 201 (1964) 68.
- [14] A.H. Kianfar, L. Keramat, M. Dostani, M. Shamsipur, M. Roushani, F. Nikpour, *Spectrochim. Acta* 77 (2010) 424.
- [15] D.N. Kumar, B.S. Garg, *Spectrochim. Acta, Part A* 59 (2006) 141.
- [16] M. Mathew, A.J. Gary, G.J. Palenik, *J. Am. Chem. Soc.* 92 (1972) 3197.
- [17] A. Pasini, M. Gulloti, *J. Coord. Chem.* 3 (1974) 319.
- [18] D.M. Boghaei, S. Mohebbi, *Tetrahedron* 58 (2002) 5357.
- [19] A.H. Sarvestani, S. Mohebbi, *J. Irnian, Chem. Soc.* 4 (2007) 215.
- [20] A.H. Sarvestani, A. Salimi, S. Mohebbi, R. Hallaj, *J. Chem. Res.* (2005) 190.
- [21] A.H. Sarvestani, S. Mohebbi, *J. Chem. Res.* (2006) 257.
- [22] E.G. Jäger, K. Schuhmann, H. Görts, *Inorg. Chem. Acta* 255 (1997) 295.
- [23] S. Zolezzi, E. Spodine, A. Decinti, *Polyhedron* 21 (2002) 55.
- [24] H.H. Jaffe, *Chem. Rev.* 53 (1953) 191.